arXiv:0709.0384v1 [cond-mat.soft] 4 Sep 2007

Thermophoresis of strongly charged colloidal particles

Sébastien Fayolle, Thomas Bickel, and Alois Würger
CPMOH, Université Bordeaux 1 & CNRS, 351 cours de la Libération, 33405 Talence, France

We present a microscopic theory for thermally driven transport in colloidal suspension of charged particles. For small valency, we recover known results from Debye-Hückel approximation, which are in quantitative agreement with recent experiments on polystyrene particles and sodium dodecyl sulphate micelles. Significant modifications occur for strong charges, where the thermodiffusion coefficient is independent of the Debye length and the permittivity of the electrolyte, but is proportional to the valency of the macroion.

PACS numbers: 66.10.Cb, 82.70.-y

I. INTRODUCTION

A thermally driven flow, or Ludwig-Soret effect, is observed when applying a thermal gradient to a complex fluid [1, 2, 3, 4]. The corresponding mass transport is relevant for natural and technological processes, such as the global circulation of sea water [5] and the phase behavior of eutectic systems at solidification [6]. In recent years, detailed experimental studies on macromolecular solutions and colloidal suspensions have revealed unambiguous and often surprising dependencies of the Soret effect on system parameters such as salinity, surface coating, solute concentration, and molecular weight [7, 8, 9, 10, 11, 12, 13, 14, 15, 16, 17, 18]. Although the analogy to electrophoresis indicates the relevance of surface or Marangoni forces and suggests a hydrodynamic treatment [19, 20], the physcial mechanisms that drive thermophoresis in liquids are poorly understood and differ from those in gaseous phases [21, 22].

Diffusion theory accounts for the particle current due to density gradient in terms of Fick's law $\mathbf{J} = -D\boldsymbol{\nabla} n$, where n is the number of suspended particles per unit volume. For a closed system the stationary state is characterized by $\mathbf{J} = 0$ and, in the absence of external forces, corresponds to a homogeneous density. Thermophoresis describes an additional flow that is driven by a temperature gradient, resulting in the total particle current

$$\mathbf{J} = -D\boldsymbol{\nabla} n - nD_T\boldsymbol{\nabla} T \ . \tag{1}$$

with the thermal diffusion coefficient D_T. Experimentally, D_T is determined by applying a temperature gradient to a uniform suspension ($\boldsymbol{\nabla} n = 0$) and by recording the initial current $\mathbf{J} = -nD_T\boldsymbol{\nabla} T$, or by measuring the density modulation $\delta n = -n(D_T/D)\delta T$ induced by a temperature inhomogeneity δT in the steady state $\mathbf{J} = 0$ [4]. The latter method gives the Soret coefficient

$$S_T = D_T/D \ . \tag{2}$$

Eq. (1) provides a macroscopic description for the particle current in terms of the "thermal forces" [23]. In a microscopic picture, one wishes to relate the kinetic coefficients D and D_T to the properties of solute and solvent. For this purpose we rewrite the particle current as the sum of two terms [24],

$$\mathbf{J} = n\mathbf{u} - \mu\boldsymbol{\nabla}\Pi \ . \tag{3}$$

The phoretic velocity $\mathbf{u}$ arises from the interactions at the solute-solvent interface and thus is a single-particle effect, whereas the remainder is due to the mutual forces exerted by the suspended particles in terms of the gradient of the osmotic pressure Π. The bare mobility $\mu = 1/(6\pi a\eta)$ depends on the solvent viscosity η and on the particle size a. Eq. (3) describes a non-uniform system and cannot be obtained from equilibrium statistical mechanics [20, 23]. The stationary state $\mathbf{J} = 0$ provides the condition of mechanical equilibrium, i.e., when all forces acting on a given particle cancel.

As an illustration, let us briefly discuss the case of an ideal gas. Because of the absence of interactions, one has $\mathbf{u} = 0$ and the osmotic pressure reads $\Pi = nk_BT$. The resulting particle current is then $\mathbf{J} = -\mu k_B(T\boldsymbol{\nabla} n + n\boldsymbol{\nabla} T)$. Comparing to Eq. (1) gives the Einstein relation $D = \mu k_B T$ as well as $D_T = \mu k_B$, with the Soret coefficient $S_T = 1/T$. This simply means that, at constant pressure, the stationary density is inversely proportional to the non-uniform temperature and that the particles accumulate in regions of lower temperature. Yet most colloidal suspensions show a considerably stronger, positive or negative, Soret effect, i.e., the thermally driven current by far exceeds that of an ideal gas and may be directed toward colder or warmer regions. These deviations express the failure of the ideal-gas picture for the solute and emphasize the importance of particle-solvent interactions.

In the present paper we discuss the Soret effect in charged colloidal suspensions; we complete the theoretical framework given in our previous work [24, 25] and extend the electrostatic part to strongly charged particles. In Sec. II we derive the single-particle velocity from the Stokes equation for the surrounding fluid, with slip boundary condition that is related to the anisotropy of the Maxwell tensor in the diffuse double layer. Sec. III gives the thermodiffusion coefficient D_T in terms of the surface stress, or Marangoni force, and the osmotic pressure. In Sec. IV we obtain the electrostatic properties of the boundary layer and, in particular, the anisotropy parameter. Sec. V compare our predictions with experimental findings and previous work, and we summarize our main results in Sec. VI.

II. HYDRODYNAMICS

The thermal forces acting on a colloidal particle and the resulting velocity cannot be obtained from a mechanical or thermodynamic potential. Thermophoresis is a hydrodynamic problem, and the particle velocity has to be derived from a fluid-mechanical treatment [20]. The thermally driven motion of micron or nanometer sized particles in a viscous liquid involves small Reynolds numbers, i.e., inertia effects are negligible. Then the stationary velocity is given by Stokes' equation [26, 27, 28]

$$\eta \nabla^2 \mathbf{v} = \boldsymbol{\nabla} P - \boldsymbol{\nabla} \cdot \mathcal{T} \ , \tag{4}$$

where η is the solvent viscosity. An incompressible fluid satisfies moreover $\boldsymbol{\nabla} \cdot \mathbf{v} = 0$ and stick boundary conditions at the particle surface, $\mathbf{v} = \mathbf{u}$. Besides the pressure gradient $\boldsymbol{\nabla} P$, the fluid is subject to the Maxwell stress tensor $\mathcal{T}_{ij}$ which, contrary to the hydrostatic pressure P, is anisotropic and thus takes different values parallel and perpendicular to the particle surface.

The force field induced by surface charges, $\boldsymbol{\nabla} \cdot \mathcal{T}$, is finite only within a boundary layer thickness λ, which is given by the Debye screening length $\lambda = \kappa^{-1}$. Throughout this paper we suppose that the thickness of the boundary layer λ is much smaller than the particle radius a,

$$\lambda \ll a \ .$$

The characteristic length scales of the normal and parallel derivatives in Eq. (4) are given by λ and a, respectively. Thus the forces vary rapidly in the normal direction, and much more slowly along the interface. This separation of length scales permits us to calculate the particle velocity in two steps, as schematically drawn in Fig. 1. First, resorting to a 1D approximation that is valid at distances much shorter than the particle size, we discuss the boundary layer and derive the surface force induced by the temperature gradient. In a second step we obtain the fluid velocity field at distances well beyond λ, where the Maxwell tensor vanishes.

A. Boundary layer

Close to particle, the surface may be considered as flat, with normal and parallel coordinates z and x. Since the electric field $\mathbf{E}$ of a uniformly charged spherical particle is normal to the surface, the Maxwell tensor is diagonal with elements $\mathcal{T}_{ii}$ where $i = x, y, z$. Then Stokes' equation reads

$$\eta \nabla^2 v_i = \partial_i (P - \mathcal{T}_{ii}) \ ,$$

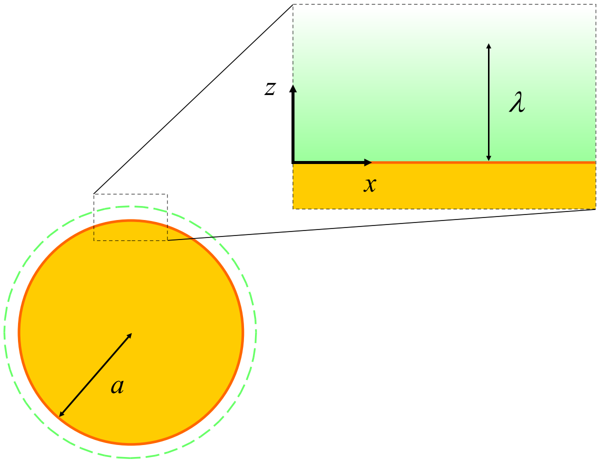

FIG. 1: (Color online) Illustration of the boundary layer approximation developed hereafter. Very close to the particle surface, a 1D approximation is valid. This solution then acts as a boundary condition for the problem at distances well beyond the layer thickness λ.

with $\partial_x = \partial/\partial x$, etc. The normal velocity vanishes close to the interface, $v_z = 0$; thus $\partial_z (P - \mathcal{T}_{zz}) = 0$ so that $P - \mathcal{T}_{zz} = P_0$ is a constant. Inserting this relation in the equation for v_x and noting that, because of the thermal gradient, v_x is slowly varying along the surface, we find

$$\eta \partial_z^2 v_x = \partial_x (\mathcal{T}_{zz} - \mathcal{T}_{xx}) \ . \tag{5}$$

The derivative on the right-hand side gives the lateral force per unit volume exerted on the fluid.

Since $\mathcal{T}$ is finite within the boundary layer only, the force density $\partial_x (\mathcal{T}_{zz} - \mathcal{T}_{xx})$ vanishes beyond a distance λ from the interface. Integrating over the normal coordinate gives the total shear stress on the fluid accumulated through the boundary layer,

$$\frac{\partial}{\partial x} \int_0^\infty dz (\mathcal{T}_{zz} - \mathcal{T}_{xx}) = - \frac{df}{dS} \ .$$

The right-hand side gives the lateral force df acting on the surface element dS of the particle.

B. Surface force on a spherical particle

Well beyond the boundary layer, the surface can no longer be taken as flat and the above approximation ceases to be valid. At distances comparable to the particle radius a, one has to deal with the 3D Stokes equation, yet with modified boundary conditions. The electric stress is absorbed in the boundary layer, and Eq. (4) simplifies to $\eta \nabla^2 \mathbf{v} = \nabla P$. It turns out convenient to define the anisotropy parameter characterizing the boundary layer

$$\gamma = \int_a^\infty dr (\mathcal{T}_\perp - \mathcal{T}_\parallel) \ , \tag{6}$$

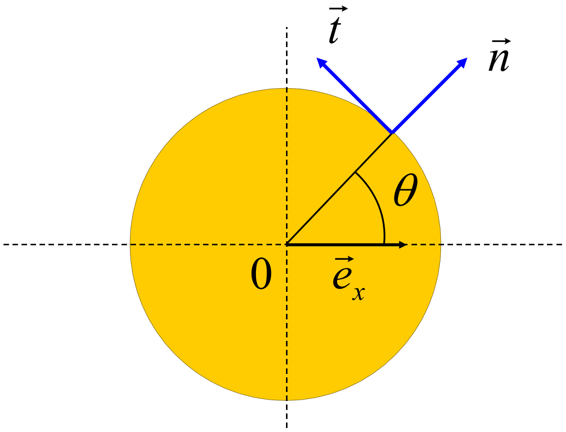

FIG. 2: (Color online) Representation of the particle with the normal and parallel directions **n** and **t**. The polar angle is noted θ.

where $\mathcal{T}_\perp$ and $\mathcal{T}_\parallel$ are the normal and parallel components of the Maxwell tensor, and where we have used $\lambda \ll a$. Then the oriented surface force reads

$$\frac{d\mathbf{f}}{dS} = -\boldsymbol{\nabla}_\parallel \gamma \ , \tag{7}$$

its direction is parallel to the particle surface and opposite to the 2D gradient $\boldsymbol{\nabla}_\parallel \gamma$. In the case of a non-uniform temperature one has

$$\boldsymbol{\nabla}_\parallel \gamma = \gamma_T \boldsymbol{\nabla}_\parallel T \ , \tag{8}$$

where we have assumed that spatial variations arises from the thermal gradient only and that the elements of the Maxwell tensor depend on temperature.

Since heat propagation is much faster than particle migration, the temperature field may be taken as stationary. Starting from the overall thermal gradient of the fluid

$$\boldsymbol{\nabla} T = T_x \mathbf{e}_x$$

with constant T_x, the heat conduction equation for a spherical particle is readily solved, and the gradient at the particle surface reads [28]

$$\boldsymbol{\nabla}_\parallel T = \xi (\mathbf{t} \cdot \boldsymbol{\nabla} T)\mathbf{t} = -\xi T_x \sin\theta \mathbf{t} \ ,$$

where the polar angle θ is given by $\sin\theta = -\mathbf{e}_x \cdot \mathbf{t}$ — see Fig. 2 for a definition of the unitary vectors **n** and **t**. The parameter

$$\xi = \frac{3\kappa_S}{2\kappa_S + \kappa_P}$$

is determined by the heat conductivities of solvent and particle.

C. Single-particle velocity

In a mesoscopic description, we may put $\lambda \to 0$ and consider $\boldsymbol{\nabla}_\parallel \gamma$ as a surface force acting at the particle-fluid interface. Thus Eq. (4) reduces to the force-free Stokes equation

$$\eta \nabla^2 \mathbf{v} = \boldsymbol{\nabla} P \ , \tag{9}$$

albeit with modified boundary conditions that account for the surface force accumulated through the boundary layer. The stress tensor

$$\boldsymbol{\sigma} = \boldsymbol{\sigma}' - P$$

comprises the dissipative term or viscous force density $\sigma'_{ij} = \eta \left(\partial_i v_j + \partial_j v_i\right)$, and the hydrostatic pressure P [28].

The stick boundary conditions of hydrodynamics, imposing a continuous velocity at the interface, $\mathbf{v}|_{r=a} = \mathbf{u}$, cease to be valid in the presence of surface forces. The fluid being incompressible, the normal component is continuous,

$$\mathbf{n} \cdot \mathbf{v}|_{r=a} = \mathbf{n} \cdot \mathbf{u} \ , \tag{10}$$

whereas the parallel velocity in general exhibits a jump. A second condition is obtained by noting that there is no net external force acting on the system consisting of the particle and the boundary layer. Thus the integrated normal force outside the boundary layer vanishes [20],

$$\oint dS \boldsymbol{\sigma} \cdot \mathbf{n} = 0 \ . \tag{11}$$

The third condition involves the surface force (8), which plays the role of the source field and imposes a finite shear stress [28],

$$\mathbf{t} \cdot (\boldsymbol{\sigma} \cdot \mathbf{n} + \boldsymbol{\nabla}_\parallel \gamma) = 0 \ . \tag{12}$$

It turns out that this condition results in a finite slip velocity.

The source term (12) differs from that of electrophoresis, where the Stokes equation in the boundary layer reads $\eta \partial_z^2 v_x = \varepsilon E_{\text{ext}} \partial_z^2 \psi$, with the external electric field E_{ext} and the local potential ψ. Integrating this equation twice, with stick boundary conditions, gives the mesoscopic slip velocity $v_S = -\varepsilon E_{\text{ext}} \psi_0 / \eta$ as a function of the surface potential ψ_0, resulting in $\mathbf{t} \cdot (\mathbf{v} - \mathbf{u})|_{r=a} = v_S$ [20]. In the case of thermophoresis, integration of Eq. (5) results in the surface stress $\boldsymbol{\nabla}_\parallel \gamma$; the slip velocity is obtained only after solving Eqs. (9)–(12).

In the laboratory frame the particle moves at a velocity $\mathbf{u} = u \mathbf{e}_x$. Transforming to the reference frame in which the particle is at rest, we have $\hat{\mathbf{u}} = 0$ and $\hat{\mathbf{v}}(\mathbf{r}) = \mathbf{v}(\mathbf{r}) - \mathbf{u}$. The solution of Stokes' equation at small Reynolds numbers in spherical coordinates $\hat{\mathbf{v}} = \hat{v}_r \mathbf{n} + \hat{v}_\theta \mathbf{t}$ reads [28]

$$\hat{v}_r = -u \cos\theta \left(1 - 2\alpha \frac{a}{r} + 2\beta \frac{a^3}{r^3}\right) \ , \tag{13a}$$

$$\hat{v}_\theta = u \sin\theta \left(1 - \alpha \frac{a}{r} - \beta \frac{a^3}{r^3}\right) \ , \tag{13b}$$

where θ is the polar angle with respect to the x axis and the radial and tangential unit vectors $\mathbf{n} = \mathbf{r}/r$ and $\mathbf{t} = \partial\mathbf{n}/\partial\theta$ satisfy $\mathbf{e}_x = \cos\theta\mathbf{n} - \sin\theta\mathbf{t}$. This flow field is related to a non-uniform hydrodynamic pressure

$$P(\mathbf{r}) = P_0 + \alpha\frac{2\eta u a}{r^2}\cos\theta\,.$$

The parameters u, α, β are determined from the solulution of Stokes' with the boundary conditions (10)–(12).

The first two of these conditions involve the fluid velocity and stress only. In the particle-fixed frame the normal velocity vanishes, $\hat{v}_r|_{r=a} = 0$, resulting in $1-2\alpha+2\beta = 0$. The total stress at the interface can be written as $\boldsymbol{\sigma}\cdot\mathbf{n} = \mathbf{n}\sigma_{rr} + \mathbf{t}\sigma_{r\theta}$, with the entries of the dissipative part in shperical coordinates [28]

$$\sigma'_{rr} = 2\eta\frac{\partial\hat{v}_r}{\partial r}, \quad \sigma'_{r\theta} = \eta\left(\frac{\partial\hat{v}_\theta}{\partial r} - \frac{\hat{v}_\theta}{r}\right)\ .$$

Integrating (11) over a sphere just outside the boundary layer gives the relation $1 - 5\alpha + 2\beta = 0$. One readily obtains the amplitudes of the velocity field varying with distance as $1/r$ and $1/r^3$, respectively,

$$\alpha = 0, \qquad \beta = -\frac{1}{2}\ . \tag{14}$$

The remaining condition (12) relates the stress $\sigma'_{r\theta}$ and the surface force and determines the particle velocity

$$u = -\frac{\xi a\gamma_T}{3\eta}T_x\ . \tag{15}$$

Finally, taking the back transformation $\mathbf{v}(\mathbf{r}) = \hat{\mathbf{v}}(\mathbf{r}) + \mathbf{u}$ yields the fluid velocity in the laboratory frame

$$\mathbf{v}(\mathbf{r}) = u\frac{a^3}{r^3}\left(\frac{1}{2}\sin\theta\mathbf{t} + \cos\theta\mathbf{n}\right)\ . \tag{16}$$

The slip velocity, i.e., the velocity change through the boundary layer, is given by the tangential component $\hat{v}_\theta(a)$,

$$\mathbf{v}_S = \frac{3}{2}u\sin\theta\mathbf{t}.$$

Its maximum value $\frac{3}{2}u$ at $\theta = \frac{\pi}{2}$ exceeds the particle velocity, which means that the particle and the fluid move in opposite directions.

Eq. (15) provides the relation the phoretic velocity $\mathbf{u}$ and the applied temperature gradient $\boldsymbol{\nabla}T = T_x\mathbf{e}_x$,

$$\mathbf{u} = -C\boldsymbol{\nabla}T\ , \tag{17}$$

with the transport coefficient

$$C = \frac{\xi a}{3\eta}\frac{d\gamma}{dT}\ . \tag{18}$$

This result displays how the phoretic velocity arises from the competition of particle-solvent interactions that drive the particle, and the fluid viscosity.

D. Mobility

Eq. (7) accounts for the balance of the stress on the fluid and the force $d\mathbf{f}$ acting on a surface element dS of the particle. Inserting the expression of $\boldsymbol{\nabla}_\parallel T$ and separating the dependence on the angle θ, we have

$$\mathbf{f} = 2\pi a^2\gamma_T\kappa T_x\int_{-1}^{1} d(\cos\theta)\sin\theta\mathbf{t}\ .$$

The integral takes the value $-\frac{4}{3}\mathbf{e}_x$, resulting in the total force

$$\mathbf{f} = -\frac{8}{3}\pi a^2\gamma_T\xi\boldsymbol{\nabla}T\ .$$

A phoretic mobility may be defined as the ratio of the one-particle velocity and the force, $\mathbf{u} = \mu_{\text{ph}}\mathbf{f}$. Comparing with (17) gives

$$\mu_{\text{ph}} = \frac{1}{8\pi\eta a}\ . \tag{19}$$

This expression differs from the mobility μ that describes a particle subject to an external force $\mathbf{F}_{\text{ext}}$ or the Brownian force leading to diffusive motion. The solution of the Stokes equation with such an external force satisfies stick boundary conditions $\mathbf{v}|_{r=a} = \mathbf{u}$ and the force balance $\mathbf{F}_{\text{ext}} + \int dS\boldsymbol{\sigma}\cdot\mathbf{n} = 0$, resulting in [28]

$$\alpha_F = \frac{3}{4},\ \ \beta_F = \frac{1}{4},\ \ u_F = \mu F_{\text{ext}},$$

the excess hydrodynamic pressure $P(\mathbf{r}) - P_0 \sim 1/r^2$, and a velocity field $\mathbf{v}_F$ that decays with distance as $v_F \sim 1/r$.

III. KINETIC COEFFICIENTS

The results of the previous section are now applied to derive general expressions for the transport coefficient D and D_T. We consider a suspension of interacting particles in an inhomogeneous temperature field $T(\mathbf{r})$, where both the density n and the osmotic pressure Π are, in general, spatially varying functions. Such a system cannot be dealt with in terms of equilibrium statistical mechanics; its steady state and the relaxational kinetics are described in terms of the particle current Eq. (3). After expressing both terms by microscopic quantities proportional to $\boldsymbol{\nabla}n$ and $\boldsymbol{\nabla}T$, we compare to Eq. (1).

A. Osmotic pressure

The particle current contains, besides the single-particle velocity $\mathbf{u}$, a term proportional to the pressure gradient $\boldsymbol{\nabla}\Pi$. The latter depends on both density and temperature modulations,

$$\boldsymbol{\nabla}\Pi = \Pi_T\boldsymbol{\nabla}T + \Pi_n\boldsymbol{\nabla}n\ . \tag{20}$$

with the shorthand notation $\Pi_T = \partial\Pi/\partial T$, etc.

For a non-uniform system with a pair interaction V, the pressure is calculated by explicitly writing the forces on a particle at position $\mathbf{r}$; proceeding as with the Clausius virial function one finds the sum of the ideal-gas pressure nk_BT and the two-particle forces $\mathbf{f}_{ij} = -\boldsymbol{\nabla}_i V(\mathbf{r}_i - \mathbf{r}_j)$ [29],

$$\Pi(\mathbf{r}) = n(\mathbf{r})k_BT(\mathbf{r}) + \frac{1}{6}\left\langle \sum_{i,j} \mathbf{r}_{ij}\cdot\mathbf{f}_{ij}\delta(\mathbf{r}-\mathbf{r}_i)\right\rangle \; .$$

Assuming the pair interaction $V(r_{ij})$ to be isotropic and sufficiently short-ranged, one has with the density-density correlation function $g(\mathbf{r},\mathbf{r}')$

$$\Pi = nk_BT - \frac{n}{6}\int dV' g(\mathbf{r},\mathbf{r}')r'\frac{dV(r')}{dr'} \; .$$

This relation is a useful starting point for a perturbative evaluation of the diffusion current in terms of temperature and density gradients.

So far we have avoided the use of equilibrium thermodynamics; the above relations involve mechanical and hydrodynamic forces only. Since D and D_T are linear-response coefficients, they may be evaluated in terms of equilibrium statistical mechanics, and $\langle\ldots\rangle$ may be considered as the canonical average with the Gibbs distribution. This means in particular that the density and temperature fields are replaced by their mean values n and T.

For dilute and weakly interacting systems, a widely used approximation consists in expanding the pressure in powers of the particle density,

$$\Pi = k_BT\left(n + Bn^2 + \ldots\right) , \qquad (21)$$

and truncating at quadratic order, with a coefficient

$$B = \frac{1}{2}\int dV\left(1 - e^{-V(r)/k_BT}\right) \qquad (22)$$

that still depends on temperature [29]. Most relevant pair interactions are repulsive, such as the screened electrostatic potential in an electrolyte and the entropic short-range repulsion due to polymers grafted on colloidal particles. Then the virial coefficient is positive, $B > 0$ and the interactions enhance the pressure.

B. Thermal diffusion coefficient

Inserting $\mathbf{u}$ and $\boldsymbol{\nabla}\Pi$ in Eq. (3) and comparing to Eq. (1) yields

$$D = \mu\Pi_n \; , \text{ and } \; D_T = \frac{\mu}{n}\Pi_T + C \; . \qquad (23)$$

Together with the virial expansion Eq. (21), the translational diffusion coefficient takes the form

$$D = \mu k_BT\left(1 + 2Bn + ...\right) \; , \qquad (24)$$

which does not depend on the temperature gradient and is insensitive to surface forces. A different picture arises for the remaining coefficient,

$$D_T = \mu k_B\left(1 + Bn + nTB_T + ...\right) + C \; , \qquad (25)$$

which depends explicitly on the temperature derivative B_T and on the surface force parameter C.

For an ideal gas both the particle-solvent potential and the pair interaction vanish, resulting in $C = 0$ and $B = 0$. One readily recovers the transport and Soret coefficients $D = \mu k_BT$, $D_T = \mu k_B$, and $S_T = 1/T$.

IV. THE ANISOTROPY PARAMETER

The above expression for the transport coefficient depends on the charged double layer through the parameter γ which characterizes the anisotropy of the Maxwell stress tensor. The electrostatic properties of the boundary layer are closely related to the distribution of the mobile co-ions and counter-ions of the electrolyte. In three dimensions, the resulting Poisson-Boltzmann (PB) equation cannot be solved analytically. Approximate solutions exist for two particular situations. First, for weak charges, the potential $e\Psi(r)$ is small as compared to the thermal energy and the PB equation can be linearized. Second, for particles that are significantly larger than the Debye length, the potential can be evaluated as an asymptotic series in terms of the small parameter

$$\epsilon = \frac{1}{\kappa a} \; . \qquad (26)$$

Since a small radius $a < \kappa^{-1}$ implies rather a weak charge, and large valencies are possible for sufficiently large particles only, the two approximations cover in fact most physical systems. In both cases, the resulting potential Ψ is an effective quantity that contains, besides the potential energy, the entropy of the mobile ions.

The limiting cases of weak and strong charges are expressed by the ratio of the bare valency Z and its effective value

$$Z^* = \frac{4(1+\kappa a)a}{\ell_B} \; , \qquad (27)$$

that is given in terms of the particle size a, the Debye screening parameter

$$\kappa = \sqrt{8\pi n_0\ell_B} \; , \qquad (28)$$

and the Bjerrum length $\ell_B = e^2/(4\pi\varepsilon k_BT)$, with ε the dielectric constant of the solvent ($\varepsilon/\varepsilon_0 \simeq 78$ for water).

A. The Poisson-Boltzmann equation

In the mean-field approximation, the electrostatic potential of a charged particle satisfies the PB equation

$$\nabla^2\Psi(\mathbf{r}) = \frac{2n_0e}{\varepsilon}\sinh\frac{e\Psi(\mathbf{r})}{k_BT} \; . \qquad (29)$$

This equation has to be solved together with the following boundary conditions. First, the potential vanishes at infinity, $\lim_{r\to\infty}\Psi(r)=0$, and second, the electric field at the surface of the colloid is related to the surface charge σ according to

$$\left.\frac{d\Psi}{dr}\right|_{r=a}=-\frac{\sigma}{\varepsilon}\ . \qquad (30)$$

However, since the PB equation is non-linear, one can only find an approximate solution in spherical geometry. We discuss below the two relevant limits of weakly charged and highly charged colloids. To proceed, it turns out convenient to define the reduced potential

$$y(r)=\frac{e\Psi(r)}{k_BT} \qquad (31)$$

that obeys the differential equation

$$\nabla^2 y=\kappa^2\sinh y\ . \qquad (32)$$

B. Debye-Hückel approximation

We first recall the electrostatic properties for weakly charged systems. In this case, the reduced potential is small everywhere, $y \ll 1$. Then Eq. (32) can be linearized, $\nabla^2 y_{\rm DH}(\mathbf{r})=\kappa^2 y_{\rm DH}(\mathbf{r})$, and solved by the well-known Debye-Hückel potential

$$y_{\rm DH}(\mathbf{r})=\frac{Z\ell_B}{1+\kappa a}\frac{e^{-\kappa(r-a)}}{r}\ . \qquad (33)$$

This solution ceases to be valid if the surface potential $y_{\rm DH}(a)$ approaches unity, i.e., if the valency Z is of the order of the effective value Z^*.

C. The multiple scale method

For highly charged particles the nonlinearities in the PB equation are essential and result in a much more intricate problem. Still, an asymptotic expansion

$$y(r)=y_0(r)+\epsilon y_1(r)+\epsilon^2 y_2(r)+\dots \qquad (34)$$

can be derived explicitly if the parameter ϵ is small, i.e., if the Debye length is smaller than the particle radius. Note that the coefficients y_n in (34) still depend on ϵ, i.e., we have not yet defined how to construct the series.

The usual boundary conditions of electrostatics impose that the potential vanishes at infinity, $\lim_{r\to\infty} y_n(r)=0$, and satisfies (30) at the particle surface. Since Eq. (30) is independent of κa, the derivative involves the term $n=0$ only

$$\left.\frac{dy_0}{dr}\right|_{r=a}=-\frac{\sigma e}{k_BT\varepsilon}\ , \qquad (35)$$

and vanishes for $n\ge 1$

$$\left.\frac{dy_n}{dr}\right|_{r=a}=0\ . \qquad (36)$$

The multiple scale approach [30] allows to systematically match the known 1D solution close to the particle surface to the screened potential at distances well beyond the Debye-Hückel length. This is achieved by introducing

$$x_1=\frac{1}{\epsilon}\left(\frac{r}{a}-1\right),\qquad x_2=\frac{r}{a}\ , \qquad (37)$$

where the "fast" variable x_1 accurately describes the problem in the vicinity of the surface, in addition to the "slow" variable x_2 which accounts for the spherical symmetry of the problem far from the particle. The derivative thus becomes $d/dr=a^{-1}(\epsilon^{-1}\partial_1+\partial_2)$, with $\partial_i=\partial/\partial x_i$, and the Laplace operator reads in terms of this new set of variables

$$\nabla^2=\partial_1^2+2\epsilon\left(\partial_1\partial_2+\frac{1}{x_1}\partial_2\right)+\epsilon^2\left(\partial_2^2+\frac{2}{x_2}\partial_2\right)\ . \qquad (38)$$

Finally we expand the $\mathcal{S}=\sinh y$ according to

$$\mathcal{S}=\mathcal{S}_0+\left(\epsilon y_1+\epsilon^2 y_2+\dots\right)\mathcal{C}_0+\frac{1}{2}\left(\epsilon y_1+\epsilon^2 y_2+\dots\right)^2\mathcal{S}_0+\dots$$

with $\mathcal{S}_0=\sinh y_0$ and $\mathcal{C}_0=\cosh y_0$. Inserting these relations in the PB equation (32), we obtain a set of coupled equation for y_n that can be solved by identifying terms of the same power of ϵ. We give explicitly the equation at order ϵ^0,

$$\partial_1^2 y_0=\sinh y_0\ , \qquad (39)$$

and that at order ϵ^1,

$$-\partial_1^2 y_1+y_1\cosh y_0=\frac{2}{x_2}\partial_1 y_0+2\partial_1\partial_2 y_0\ . \qquad (40)$$

1. *Zeroth-order solution y_0*

At lowest order in ϵ the differential equation (39) can be integrated as [31]

$$\partial_1 y_0=-2\sinh\frac{y_0}{2}$$

where we have used the condition $y_0\to 0$ and $\partial_1 y_0\to 0$ as $x_1\to\infty$. This equation can be integrated once more and one finds [31]

$$y_0=2\ln\frac{1+f\left(x_2\right)e^{-x_1}}{1-f\left(x_2\right)e^{-x_1}}$$

where the unknown integration function $f(x_2)$ remains to be determined.

The point is now that we artificially introduced an extra variable in the problem. The equation of order ϵ^0 and the boundary conditions at $r = a$ and $r \to \infty$ are not sufficient to obtain the function of two variables $y_0(x_1, x_2)$. Following [32], we thus require that the non homogeneous part of Eq. (40) for the *first order* solution decays faster than $\exp[-x_1]$. Explicitly, this requirement reads

$$x_2 \partial_2 f(x_2) + f(x_2) = 0$$

so that $f(x_2) = g_0/x_2$, with g_0 constant.

Coming back to the original variable, the lowest order term of the expansion reads

$$y_0(r) = 2 \ln \frac{1 + g(r)}{1 - g(r)} \ , \tag{41}$$

with

$$g(r) = g_0 \frac{a}{r} \exp\left[-\kappa\left(r - a\right)\right] \ . \tag{42}$$

The integration constant g_0 is finally obtained from the boundary condition (35)

$$g_0 = -\frac{1}{p} + \sqrt{1 + \frac{1}{p^2}}, \qquad p = \frac{2Z}{Z^*} \ . \tag{43}$$

To leading order in $1/(\kappa a)$, the parameter p may be written as $p = \kappa^{-1}/\ell_{GC}$, i.e., the ratio of Debye and Gouy-Chapman lengths κ^{-1} and $\ell_{GC} = 1/(2\pi\sigma\ell_B)$.

2. *Small valency $Z \ll Z^*$*

If $p \ll 1$, one has $g_0 \simeq p/2$ and the solution (41) reduces to

$$y_0(r) = \frac{Z\ell_B}{1 + \kappa a} \frac{e^{-\kappa(r-a)}}{r} \ . \tag{44}$$

As expected, we recover the Debye-Hückel solution for weakly charged colloids.

3. *High valencies $Z \gg Z^*$*

In the limit $p \gg 1$, the solution y_0 exhibits quite different behaviors at short and long distances. In the latter case, one recovers well beyond the Debye length, $\kappa(r - a) \gg 1$, the screened potential

$$y_0(r) = \frac{Z^*\ell_B}{1 + \kappa a} \frac{e^{-\kappa(r-a)}}{r} \ , \tag{45}$$

albeit with the effective valency Z^*. Close to the surface of the particle, $\kappa(r - a) \ll 1$, the potential simplifies to a logarithmic law

$$y_0(r) = -2 \ln \kappa(r - a) \ . \tag{46}$$

4. *Higher order corrections*

Higher order terms in the expansion can be evaluated following the same method. We give below only the first order correction, which is obtained by solving Eq. (40) together with the requirement that the non homogeneous part of the equation for y_2 does not contains terms proportional to $\exp[-x_1]$. We obtain

$$y_1(r) = -\frac{2g(r)}{1 - g(r)^2} \left[\frac{a}{r} g(r)^2 + k\right] \ .$$

The constant k is obtained by enforcing the boundary condition at the surface of the particle $\left(\partial y_1/\partial r\right)_{r=a} = 0$. Explicitly, we find

$$k = \frac{(1 + 2\epsilon)\, g_0^4 - (3 + 4\epsilon)\, g_0^2}{(1 + g_0^2)\,(1 + \epsilon)} \ .$$

Expanding this expression at lowest order in ϵ, one recovers the result of Ref. [32]. Incidentally, we note that the effective charge obtained from the behavior of the potential in the limit $p \gg 1$ is now corrected to become $Z^* = \frac{4a}{\ell_B}(\frac{3}{2} + \kappa a)$, as pointed out by Trizac and collaborators [33]. This correction is, however, irrelevant in the limit $\kappa a \gg 1$ considered here. Contributions of quadratic and higher order in ϵ can be obtained by repeating the same procedure.

D. The anisotropy parameter

In view of Eq.(6), we now evaluate the Maxwell stress tensor which is given by the components of the electric field $\mathbf{E} = -\boldsymbol{\nabla}\Psi$,

$$\mathcal{T}_{ij} = \varepsilon \left(E_i E_j - \frac{1}{2}\delta_{ij}\mathbf{E}^2\right) \ .$$

Since the electric field of a spherical particle is normal to the surface, the off-diagonal or shear components vanish; the diagonal elements are finite, the normal one being positive and the two parallel to the surface negative,

$$\mathcal{T}_\perp = \frac{\varepsilon}{2} E^2 = -\mathcal{T}_\parallel \ .$$

In the limit $\kappa a \gg 1$ the particle surface may be considered as flat, and the anisotropy parameter (6) reads

$$\gamma = \varepsilon \int_a^\infty dr E(\mathbf{r})^2 \ .$$

Inserting y_0 one obtains $\gamma = \varepsilon(k_B T/e)^2 \int dr\, (dy_0/dr)^2$. Replacing the valencies by the charge number densities

$$\sigma = \frac{Z}{4\pi a^2}, \quad \sigma^* = \frac{Z^*}{4\pi a^2} = \frac{\kappa}{\pi \ell_B} \ ,$$

we find

$$\gamma = k_B T \left(\sqrt{4\sigma^2 + \sigma^{*2}} - \sigma^*\right) \ . \tag{47}$$

In the two limiting cases with respect to the ratio σ/σ^* one has

$$\gamma = \begin{cases} 2k_BT\sigma^2/\sigma^* & \text{for} \quad \sigma \ll \sigma^* \ , \\ 2k_BT\sigma & \text{for} \quad \sigma^* \ll \sigma \ . \end{cases} \tag{48}$$

The effective charge density σ^* depends on temperature, whereas the bare value σ is constant. In an inhomogeneous system, $T(\mathbf{r})$ is slowly varying along the interface, and σ^* and γ are well defined local quantities.

The derivative γ_T is calculated by rewriting the effective charge density as $\sigma^* = (\kappa/\pi\ell_B)$ and by noting the dependencies of Debye and Bjerrum lengths, $\kappa^{-1} \propto \sqrt{\varepsilon T}$ and $\ell_B \propto 1/(\varepsilon T)$, and of the dielectric constant ε [34]

$$\alpha = -\frac{d\ln\varepsilon}{d\ln T} \ .$$

Thus one finds the relation $d\sigma^*/dT = (1-\alpha)\sigma^*/2T$, and finally obtains

$$\frac{d\gamma}{dT} = \frac{\gamma}{2T}\left(2 - \frac{\sigma^*}{\sqrt{4\sigma^2 + \sigma^{*2}}}(1-\alpha)\right) \ . \tag{49}$$

At room temperature the parameter α takes the value $\alpha = 1.4$.

In the limit of weak charges one has $\gamma_T = \frac{1}{2}(\gamma/T)(1+\alpha)$ and thus recovers the expression given previously in [24]

$$\gamma_T = k_B(1+\alpha)\frac{\sigma^2}{\sigma^*} \quad \text{for} \quad \sigma \ll \sigma^* \ , \tag{50}$$

whereas in the opposite case we find

$$\gamma_T = 2k_B\sigma \quad \text{for} \quad \sigma^* \ll \sigma \ . \tag{51}$$

These expressions for the parameter γ_T constitute a main result of the present paper; with Eqs. (18) and (25) they provides the explicit form of the thermodiffusion coefficient D_T.

V. DISCUSSION

The preceding sections provide an explicit expression for the thermally driven particle current

$$\mathbf{J}_{\text{th}} = -nD_T\nabla T \ ,$$

which according to Eq. (25) consists of two contributions; the first one, $n\mu k_B\nabla T$, describes a diffusive current due to the non-uniform stationary state in a temperature gradient, whereas the second one, $nC\nabla T$, arises from surface forces. The latter contribution is proportional to the parameter γ_T calculated above.

In this section we discuss the relative magnitude of these contributions, their dependencies on physical parameters of the solute and the solvent, and compare our results with experimental findings and previous theoretical work. We mostly consider the dilute limit, where

$$D_T = \mu k_B + C \ .$$

Interaction effects that occur at higher densities are addressed separately.

A. Dominant driving force

It is instructive to estimate the relative magnitude of the two contributions to D_T, that is the ratio

$$\frac{C}{\mu k_B} = \xi\frac{4\pi a^2\gamma_T}{k_B} \ . \tag{52}$$

This quantity exceeds unity for most experimentally relevant systems. Thus for micron-sized polystyrene beads with typical parameters $a \approx 1$ μm, $\sigma \approx 10^{-2}$ e/nm^2, $\kappa^{-1} \approx 10$ nm, and the viscosity and permittivity of water [18], one finds the value $C/\mu k_B \approx 10^3$. Even for solutes in the nanometer range, this ratio may be large; for instance in the case of sodium dodecyl sulphate (SDS) micelles of valency $Z \approx 30$ and radius $a \approx 3$ nm [12], the resulting ratio $C/\mu k_B$ lies between 1 and 10. Note that we have used here $\xi \approx 1$, which holds for most colloidal suspensions.

Similar arguments hold for polymer solutions, where the monomer-solvent interaction is at least of the order k_BT. The phoretic coefficient $C \sim k_B/\eta a$ scales with the inverse monomer size a, whereas the mobility $\mu \sim 1/(\eta R)$ involves the gyration radius $R \sim N^\nu a$, resulting in $C/\mu k_B \sim N^\nu \gg 1$ [24].

Thus we are led to the important conclusion that for solutes larger than a few nanometers, thermal diffusion is in general driven by surface forces, i.e.,

$$D_T \simeq C \ . \tag{53}$$

This statement is confirmed by the experimental observation that hardly any system satisfies the ratio $D_T/D = 1/T$ expected for diffusive thermal transport. In physical terms this means that the ideal-gas or entropic contribution μk_B is much smaller than the surface force term C that arises from solute-solvent interactions. Note also that γ_T is always positive for the electric double layer, which means $C > 0$ and a thermophoretic current toward colder regions.

B. Particle size

In the range of parameters considered in this paper, $\kappa a \gg 1$, the parameter σ^* is independent of the particle size, and so are the surface energy γ and its derivative γ_T. As a consequence, the phoretic coefficient C varies linearly with the particle size,

$$C \propto a \ . \tag{54}$$

The stationary velocity $\mathbf{u} = -C\boldsymbol{\nabla}T$ is thus proportional to a, whereas the diffusive contribution $\mathbf{u} = -\mu k_B\boldsymbol{\nabla}T$ varies as $1/a$.

C. Surface charge and Debye length

For the case of weakly charged surfaces $\sigma \ll \sigma^*$, one finds from Eq. (50) that the phoretic coefficient C varies

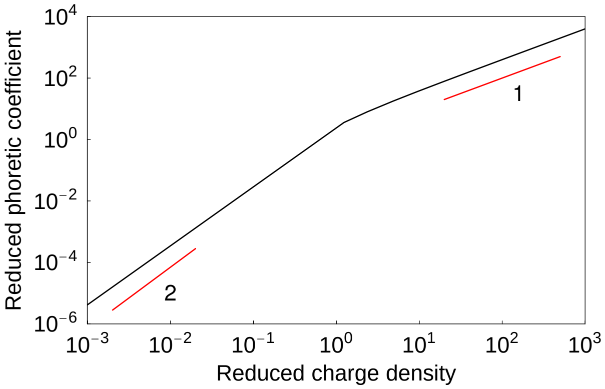

FIG. 3: Reduced phoretic coefficient $(3\eta C)/(2k_B\sigma^*\xi a)$ as a function of the reduced charge density σ/σ^*. The behavior of the phoretic coefficient switches from quadratic at low charge density to linear at high charge density.

quadratically with the charge density

$$C = \frac{\xi e^2}{12\eta T\varepsilon}\,(1+\alpha)\,\sigma^2 a\kappa^{-1} \qquad (\sigma \ll \sigma^*) \tag{55}$$

Moreover, C is proportional to the particle size a and to the Debye screening length κ^{-1}. Both dependencies on a and $\lambda = \kappa^{-1}$ are confirmed by experiment, as discussed below for the Soret coefficient.

In the opposite limit of strongly charged particles, the phoretic coefficient

$$C = \frac{2\xi k_B}{3\eta}\sigma a \qquad (\sigma \gg \sigma^*) \tag{56}$$

varies linearly with the surface charge density and with the particle size, but is independent of the Debye length and the dielectric constant of the electrolyte. The dependence with the reduced charge density σ/σ^* is shown on Fig. 3.

D. Soret coefficient

For the case of small valencies $\sigma \ll \sigma^*$, the Soret coefficient reads

$$S_T = \frac{1}{T}\left(1 + \frac{\xi}{2}\frac{\pi(e\sigma)^2}{\varepsilon k_B T}a^2\lambda\right) \ . \tag{57}$$

As discussed below, the ideal-gas value $1/T$ is small for particles larger than nanometers and may be safely neglected. The Soret coefficient is given by the remaining charge term.

The power laws $S_T \propto a^2$ and $S_T \propto \lambda$, as first predicted in [25] with $Z = 4\pi a^2\sigma$, have been confirmed recently in experiments on polystyrene beads in the parameter range $a = 100\ldots550$ nm and $\lambda = 2\ldots13$ nm [18, 35]. These dependencies may be combined to an interaction volume $4\pi a^2\lambda$, i.e., a spherical shell of thickness λ and mean radius a, thus giving clear evidence for surface forces operating in a boundary layer at the particle surface.

In the limit $\sigma \gg \sigma^*$, the Soret coefficient reduces to

$$S_T = \frac{1+\xi 4\pi\sigma a^2}{T} = \frac{1+\xi Z}{T} \ . \tag{58}$$

For large valencies one has the particularly simple form $S_T = \xi Z/T$.

E. Interaction effects

Now we turn to higher particle densities where the first correction of the virial expansion is no longer small. Although the surface-force driven coefficient C does not depend on density, the diffusion coefficient varies as $D = \mu k_B T(1 + 2nB)$. Thus for a repulsive pair interaction the Soret coefficient decreases as a function of the density

$$S_T(n) = \frac{S_T(n=0)}{1+2nB} \ . \tag{59}$$

As shown in Appendix A, the virial coefficient B depends on the Debye length λ, which in turn depends on the electrolyte strength as $\lambda \propto n_0^{-1/2}$. At high salinity, one has $a \gg \lambda$, resulting in strong screening of the electrostatic interaction and the excluded volume of hard spheres, i.e., $2B = \frac{4\pi}{3}(2a)^3$. In the dilute limit or at high salinity, the Soret coefficient is proportional to λ and thus varies as

$$S_T \sim n_0^{-1/2} \qquad \text{(low density)} \ .$$

As salinity decreases, the Debye length increases, and so does B. If the screening length becomes comparable to the particle size, $a \sim \lambda$, the virial coefficient varies as $B \sim n_0^{-3/2}$. As a consequence, for a dense suspension in a weak electrolyte, the above behavior is modified by the virial coefficient, and the Soret coefficient increases with salinity,

$$S_T \sim n_0 \qquad \text{(high density)} \ .$$

Both dependencies on n and n_0 have been, at least qualitatively, observed for SDS micelles in aqueous solution [12]. The inverse coefficient $1/S_T$ coefficient has been shown to vary linearly with density, and its slope to decrease as salinity augments, like the factor $2B$ above. Moreover, Fig. 1 of Ref. [12] reveals that in the dilute limit, increasing the salinity reduces the Soret effect, whereas for the dense micelle suspension S_T increases when adding salt. These experimental findings agree almost quantitatively with our theoretical expressions. A more detailed comparison is not an easy undertaking, since both the size and the charge of the micelles slightly vary with the electrolyte strength. Also, part of the data are in the range $a \sim \lambda$ whereas the present work relies on $a \gg \lambda$.

F. Negative Soret effect

The charged double layer is predicted to result in a "normal" Soret effect $S_T > 0$, that is, the particles drift in the direction opposite to the thermal gradient and thus accumulate in colder regions of the sample. There are, however, systems that show a more complex behavior. Aqueous suspensions of maghemite particles present an inverse Soret effect $S_T < 0$, whereas the normal behavior has been observed in organic solvents [16]. Also, the Soret coefficient of macromolecular solutions of lysozyme [13] or DNA [18] changes sign as a function of temperature and salinity. Especially these latter examples strongly suggest that the observed transport coefficient D_T comprises contributions of different physical origin and of opposite sign.

Fig. 3a of Ref. [18] displays particularly instructive data for the Soret coefficient of polystyrene beads as a function of the Debye length λ at different temperatures. S_T varies linearly with λ, as expected from (57), yet does not vanish at $\lambda = 0$; the finite intercept is negative at 6°C, increases with temperature, and changes sign at about 20°C. These observations give evidence for an additional contribution S_T' that is insensitive to charge effects but strongly temperature-dependent. A similar behavior has been reported for macromolecular suspensions [13, 18].

These experimental findings indicate that, besides the Maxwell stress tensor of the charged double layer, additional forces operate at the particle surface [36, 37]. For micron sized solutes, solid-fluid interface tension and grafted surfactant molecules contribute to the anisotropy parameter γ. A very rough estimate for the tension may be obtained from the phenomenological law $\gamma_I = \gamma_0(1 - T/T_0)$ for its temperature dependence. With parameters $\gamma_0 \approx 10$ mN/m and $T_0 \approx 10^4$ K, the force parameter $d\gamma_I/dT$ would by far exceed the double-layer contribution. Yet one should be aware that the actual situation at solid-fluid interfaces, especially at polar ones, is significantly more complex than suggested by the simple relation $d\gamma_I/dT = -\gamma_0/T_0$. Moreover, because of the short range of dispersion forces, the resulting stress anisotropy occurs in a narrow layer of about one nanometer thickness. Macroscopic hydrodynamics with constant viscosity may well not apply at such short distances.

G. Comparison with previous work

Finally, we want to compare our analysis with previous work. In the spirit of Refs. [1, 20], our description of thermophoresis relies on hydrodynamics at low Reynolds numbers. In this approach, the temperature dependence of the Maxwell tensor results in a shear stress parallel to the surface, and the force acting on the particle is given by the stress accumulated through the boundary layer. Solving Stokes' equation with the appropriate boundary condition, one obtains the velocity of the particle and the flow of the surrounding fluid.

A different route has been taken by several authors in the past few years [18, 25, 35, 38]. In those works, the driving force is related to the gradient of the effective energy W of the charged double layer,

$$\mathbf{F} = -\boldsymbol{\nabla} W = -\frac{dW}{dT}\boldsymbol{\nabla} T \ . \qquad (60)$$

This expression relies on the assumption that W may be treated like an external potential. The phoretic velocity is obtained from the steady state where the "external" force $\mathbf{F}$ and the Stokes drag $\mathbf{F}_S = -6\pi\eta a\mathbf{u}$ cancel, resulting in $\mathbf{u} = -\mu(dW/dT)\boldsymbol{\nabla} T$ and in the thermodiffusion coefficient

$$S_T = \frac{1}{T}\left(1 + \frac{1}{k_B}\frac{dW}{dT}\right) \ . \qquad (61)$$

Comparison with Eqs. (57) and (58) reveals several discrepancies which we discuss briefly.

At small valencies the double-layer free energy and the integrated anisotropy parameter γ turn out to be identical,

$$W = 4\pi a^2\gamma \qquad (Z \ll Z^*) \ .$$

Eq. (B3) of Appendix B leads to the Soret coefficient $S_T = \left(1 + 4\pi^2\sigma^2\ell_B a^2\lambda\right)/T$. Comparing with Eq. (57) shows that the charge terms obtained from hydrodynamics and from the external-force picture differ by a factor

$$\frac{\xi}{2} = \frac{1}{2}\frac{3\kappa_S}{2\kappa_S + \kappa_P} \ .$$

The parameter ξ accounts for the local modification of the temperature gradient due to the different heat conductivities of solvent and particle. For $\kappa_S = \kappa_P$ one has $\xi = 1$ and a constant gradient $\boldsymbol{\nabla} T = T_x\mathbf{e}_x$, whereas $\kappa_S \ll \kappa_P$ flattens the temperature profile around the particle and thus significantly reduces thermal transport. The latter case is relevant for suspensions of crystalline particles, where the large heat conductivity indeed suppresses thermophoresis.

The remaining factor $\frac{1}{2}$ occurring in the hydrodynamic treatment is related to the shape of the particle. For a prolate particle oriented along the thermal gradient, this factor increases, whereas it is reduced for an oblate shape. This dependency could be relevant for suspended rods, such as DNA with a persistence length exceeding the size of the molecule. Although it misses the numerical prefactor $\xi/2$, the picture of an external force provides, for weak charges, qualitatively correct results.

An additional discrepancy arises in the limit of high valencies. Comparing the charging energy W and the anisotropy parameter $4\pi a^2\gamma = 2Zk_BT$ reveals, that they differ by a logarithmic factor $\ln Z$. Thus using W for strongly charged particles results in overestimating the Soret coefficient by a factor $\sim \ln Z$.

From a more formal point of view, Eq. (60) suffers from two major shortcomings. First, since the entropy S of a classical system is defined with respect to an arbitrary reference value S_0 only, the free energy $F = U - T(S - S_0)$ comprises an arbitrary constant S_0, and its the absolute value of $dF/dT = S_0 - S$ does not carry physical information. This problem persists for the charging energy W. Since W is defined with respect to the state where the excess charges are at infinity; yet this reference state comprises the entropy of the mobile ions, which results in an arbitrary contribution to the derivative dW/dT.

A second shortcoming occurs when applying (60) to polymer solutions and dense colloidal suspensions. Since the thermally induced surface stress (7) is treated as an external force [18, 25, 35, 38], the resulting flow field $\mathbf{v}(\mathbf{r})$ comprises, contrary to Eq. (16), a term $\sim 1/r$ that would result in long-range hydrodynamic interactions [24]. As a consequence, for a particle suspension of volume fraction ϕ, one would find a reduced value $(1 - \zeta\phi)D_T$ with $\zeta \sim 1$ [39, 40], which is, however, an artefact of the external-force picture. An even more serious discrepancy arises for polymers, where (61) leads to underestimate the thermophoretic current by a factor $N^{-\nu}$, with the number of monomers N and the exponent $\nu \sim \frac{1}{2} \ldots \frac{3}{5}$ [41]. The correct treatment of the surface stress gives $\mathbf{v}(\mathbf{r}) \sim 1/r^3$ as in (16), i.e., there are no long-range hydrodynamic interactions.

Still, the Debye-Hückel approximation (B3) provides a correct description for dilute suspensions of weakly charged particles [18, 25, 35]. Given the uncertainty of the surface charge density, the missing numerical prefactor $\frac{1}{2}\xi$ is of little practical consequence.

VI. SUMMARY

Starting from Stokes' equation with a force term arising from the electric stress in diffuse double layer, we have obtained the thermodiffusion coefficient D_T for charged colloidal particles. We briefly summarize our main results.

(i) In the limit of small valencies we confirm previous work obtained in Debye-Hückel approximation. Novel results arise for strong charges, where the Soret coefficient $S_T = \xi Z/T$ is proportional to the ratio of thermal conductivities ξ and the valency Z only.

(ii) The coefficient $D_T \propto a$ is proportional to the particle size, for weak charges it is moreover linear in the Debye length λ. For strong charges, however, D_T does not vary with λ; in this range the Soret effect does not depend on the salinity nor on the permittivity of the electrolyte.

(iii) Comparing the charging energy W and the integrated anisotropy parameter $4\pi a^2\gamma$ of the Maxwell stress tensor, we find that these quantities coincide for weak valencies, which explains the qualitatively correct results obtained from the simple external-force picture of Eq. (60). Yet significant discrepancies arise in the opposite case of high valencies, where $4\pi a^2\gamma = 2Zk_BT$ results in linear behavior $S_T \sim Z$. In this range W carries a logarithmic factor $\sim \ln Z$. The resulting ambiguities would alter the Soret coefficient obtained from (61), and illustrate the need of a rigorous treatment.

Acknowledgments

The authors thank E. Trizac for helpful remarks. A.W. acknowledges stimulating discussions with W. Köhler and S. Semenov.

APPENDIX A: INTERACTING PARTICLES

In view of the expressions for the diffusion coefficients D we evaluate the virial coefficient B for charged particles in a simple approximation. A "particle" consists of one colloidal macro-ion and its diffuse cloud of counterions and co-ions. For repulsive potentials, the coefficient B accounts for an excluded volume and is expressed in terms of an effective particle radius r_0 that is larger than a.

At distances r well beyond the Debye length, the pair interaction $V(r)$ of two colloidal particles is given by the electrostatic energy of the first one in the Debye-Hückel potential of the second,

$$V(r) = k_BT \frac{\bar{Z}^2}{(1 + a/\lambda)^2} \frac{\ell_B}{r} e^{-(r-2a)/\lambda} . \tag{A1}$$

Here $\bar{Z}$ indicates the bare valency if $Z \ll Z^*$, and $\bar{Z} = Z^*$ in the opposite case.

Since the virial coefficient B cannot be evaluated as it stands, we resort to an approximation that consists in replacing the integral in (22) by an excluded volume

$$B = \frac{2\pi}{3} r_0^3 ,$$

where r_0 is the effective particle radius.

Since the particle may be considered as a rigid body, r_0 is always larger than a, thus accounting for the repulsive interaction. We define the effective radius as the distance where the pair potential is equal to the thermal energy,

$$V(r_0) = k_BT .$$

Indeed, the neighbors hardly penetrate in a region of size r_0 about a given particle, whereas they move rather freely in the remaining space. From the expression of the pair potential $V(r)$ one finds

$$r_0 = 2\left(a + \chi\lambda\right) , \tag{A2}$$

where the quantity

$$\chi = \ln\left(\frac{\bar{Z}}{1 + a/\lambda}\sqrt{\frac{\ell_B}{r_0}}\right)$$

closes an implicit equation for r_0. In the absence of interactions, or at very high salinity ($\lambda \rightarrow 0$), the excluded-volume radius is twice the particle size, $r_0 = 2a$. The enhancement due to the electrostatic repulsion is of the order of the Debye screening length. With typical parameters for SDS micelles, $\bar{Z} = 40$, $\lambda = 1$ nm, $a = 3$ nm, one finds a logarithmic prefactor of the order $\chi \sim 3$.

APPENDIX B: THE DOUBLE-LAYER FREE ENERGY

The mean-field free energy of the charged double layer is usually given in terms of the "charging energy" , i.e., the work required to assemble the charge $Q = 4\pi a^2 e\sigma$ on the particle from infinity,

$$W = 4\pi a^2 e \int_0^\sigma d\sigma' \Psi_{\sigma'}(a) \ . \qquad \text{(B1)}$$

In terms of the reduced potential y_0 given in (41), we find with $4\pi a^2\sigma = Z$

$$W = k_B T \int_0^Z dZ' y_0(a) \ .$$

Elementary integration gives

$$W = 2Zk_BT\left(\ln\frac{p+\tilde{p}}{p-\tilde{p}} - \frac{\tilde{p}}{p}\right) \qquad \text{(B2)}$$

with the shorthand notation $\tilde{p} = \sqrt{p^2+1}-1$. In the limiting cases with respect to the ratio of bare and effective valencies this expression simplifies to

$$W = \begin{cases} 2(Z^2/Z^*)k_BT & \text{for } \ Z \ll Z^* \\ 2Zk_BT\ln(4Z/Z^*) & \text{for } \ Z^* \ll Z \end{cases} . \qquad \text{(B3)}$$

[1] N. O. Young, J. S. Goldstein, and M. J. Block, J. Fluid Mech. **6**, 350 (1959).
[2] J. C. Giddings, K. D. Caldwell, and M. N. Myers, Macromolecules **9**, 106 (1976); M. E. Schimpf and J. C. Giddings, Macromolecules **20**, 1561 (1987).
[3] M. Giglio and A. Vendramini, Phys. Rev. Lett. **38**, 26 (1977).
[4] W. Köhler, S. Wiegand (Eds.), *Thermal nonequilibrium phenomena in fluid mixtures*, Lecture Notes in Physics, Vol. 584 (Springer, 2001).
[5] D. R. Caldwell and S. A. Eide, Deep-Sea Res., **28**, 1605 (1981); **32**, 965 (1985).
[6] L. L. Zheng, D. J. Larson Jr., and H. Zhang, J. Cryst. Growth **191**, 243 (1998).
[7] K. J. Zhang, M. E. Briggs, R. W. Gammon, J. V. Sengers, and J. F. Douglas, J. Chem. Phys. **111**, 2270 (1999).
[8] J. Rauch and W. Köhler, Phys. Rev. Lett. **88**, 185901 (2002).
[9] J. Rauch and W. Köhler, Macromolecules **38**, 3571 (2005).
[10] S. Wiegand, J. Phys.: Condens. Matter **16**, R357 (2004).
[11] D. Braun and A. Libchaber, Phys. Rev. Lett. **89**, 188103 (2002); S. Duhr and D. Braun, Phys. Rev. Lett. **97**, 038103 (2006).
[12] R. Piazza and A. Guarino, Phys. Rev. Lett. **88**, 208302 (2002).
[13] S. Iacopini and R. Piazza, Europhys. Lett. **63**, 247 (2003).
[14] B.-J. de Gans, R. Kita, S. Wiegand, and J. Luettmer-Strathmann, Phys. Rev. Lett. **91**, 245501 (2003).
[15] R. Kita, S. Wiegand, and J. Luettmer-Strathmann, J. Chem. Phys. **121**, 3874 (2004).
[16] G. Demouchy, A. Mezulis, A. Bee, D. Talbot, J.-C. Bacri, and A. Bourdon, J. Phys. D: Appl. Phys. **37**, 1417 (2004).
[17] S. Duhr and D. Braun, Appl. Phys. Lett. **86**, 131921 (2005).
[18] S. Duhr and D. Braun, Phys. Rev. Lett. **96**, 168301 (2006); Proc. Natl. Acad. Sci. (USA) **103**, 19678 (2006).
[19] E. Ruckenstein, J. Colloid Interface Sci. **83**, 77 (1981).
[20] J. L. Anderson, Ann. Rev. Fluid Mech. **21**, 61 (1989).
[21] F. Zheng, Adv. Colloid Interface Sci. **77**, 255 (2002).
[22] A. Mohan and H. Brenner, Phys. Fluids **17**, 038107 (2005).
[23] S. R. de Groot and P. Mazur, *Non-equilibrium thermodynamics* (North Holland Publishing, Amsterdam, 1962).
[24] A. Würger, Phys. Rev. Lett. **98**, 138301 (2007).
[25] S. Fayolle, T. Bickel, S. Le Boiteux, and A. Würger, Phys. Rev. Lett. **95**, 208301 (2005).
[26] V. G. Levich and V. S. Krylov, Ann. Rev. Fluid Mech. **1**, 293 (1969).
[27] H. Brenner, J. Colloid Interface Sci. **68**, 422 (1979).
[28] L. D. Landau and E. M. Lifshitz, *Fluid Mechanics* (Elsevier, 1987).
[29] F. Reif, *Fundamentals of Statistical and Thermal Physics* (McGraw-Hill, 1965).
[30] A. Nayfeh, *Perturbation Methods* (John Wiley and Sons, New York, 1973).
[31] E. J. W. Vervey and J. Th. G. Overbeek, *Theory of the stability of lyophobic colloids* (Elsevier, 1948).
[32] A. Shkel, O. V. Tsodikov, and M. T. Record Jr., J. Phys. Chem. B **104**, 5161 (2000).
[33] E. Trizac, M. Aubouy, and L. Bocquet, J. Phys.: Condens. Matter **15**, S291 (2003).
[34] M. Deserno and C. Holm, in : *Electrostatic Effects in Soft Matter and Biophysics* (Kluwer, Dordrecht, 2001).
[35] J. K. G. Dhont, S. Wiegand, S. Dhur, and D. Braun, Langmuir **23**, 1674 (2007).
[36] S. N. Semenov and M. Schimpf, Phys. Rev. E **69**, 011201 (2004).
[37] M.-S. Han, J. Colloid Interface Sci. **284**, 339 (2005).
[38] E. Bringuier and A. Bourdon, Phys. Rev. E **67**, 011404 (2003).
[39] W. B. Russell, D. A. Saville, and W. R. Schowalter, *Coloidal Dispersions* (Cambridge University Press, 1989).
[40] J. K. G. Dhont, J. Chem. Phys. **120**, 1632 and 1642 (2004); H. Ning, J. Buitenhuis, J. K. G. Dhont, and S. Wiegand, J. Chem. Phys. **125**, 204911 (2006).
[41] F. Brochard and P.-G. de Gennes, C. R. Acad. Sc. Paris, Série II **293**, 72 (1981).